UNCLASSIFIED

Defense Technical Information Center Compilation Part Notice

ADP015941

TITLE: Corrosion Behavior of Friction Stir Welded High Strength Aluminum Alloys

DISTRIBUTION: Approved for public release, distribution unlimited

This paper is part of the following report:

TITLE: Tri-Service Corrosion Conference

To order the complete compilation report, use: ADA426685

The following component part numbers comprise the compilation report:
ADP015920 thru ADP016031

UNCLASSIFIED

Corrosion Behavior of Friction Stir Welded High Strength Aluminum Alloys

J. B. Lumsden, M. W. Mahoney, and G. A. Pollock
Rockwell Scientific, 1049 Camino dos Rios, Thousand Oaks, CA 91360, USA

ABTRACT

Friction stir welding (FSW), a relatively new solid state joining process, is used to join aluminum alloys of all compositions including alloys essentially considered unweldable. During FSW, a rotating tool provides a continual hot working action, plasticizing metal within a narrow zone at the join line, while transporting metal from the leading face of the probe to the trailing edge as the tool moves along the interface. Although melting does not occur during FSW, temperatures are sufficiently high and times at temperature sufficiently long to cause dissolution, nucleation, and/or coarsening of strengthening precipitates. The temperature-time profile changes with distance from the nugget causing a gradient in microstructure and precipitate morphology. The altered microstructure in the weld zone becomes sensitized in some high strength aluminum alloys. Results presented assess the pitting, intergranular, and SCC corrosion behavior of FSW 7XXX and 2XXX alloys. Progress in understanding the changes in microstructure responsible for the sensitization will be discussed. The presentation also will include evaluations of approaches for corrective measures.

INTRODUCTION

Friction stir welding (FSW) is a solid state joining process invented at TWI in 1991. This technology makes it possible to join aluminum alloys, which are difficult or impossible to weld by conventional techniques.[1-10] FSW does not require expensive, sophisticated machinery or operators with highly specialized skills. It is environmentally friendly and does not need shielding gas, large power supplies, protection against radiation, or generate toxic welding fumes. The process can be completely automated and replace labor intensive mechanical joining and welding procedures. In addition, substantial weight savings can be realized by elimination of rivets and fasteners.

A schematic illustration of the FSW process is shown in Figure 1. To friction stir weld either a butt or lap joint, a specially designed cylindrical tool is rotated and plunged into the joint line. The tool has a small diameter entry probe with a concentric larger diameter shoulder. When descended to the part, the rotating entry probe contacts the surface and rapidly heats and softens a small column of metal. As the probe penetrates beneath the surface, part of this metal column is extruded above the surface. The tool shoulder and length of probe control the penetration depth.

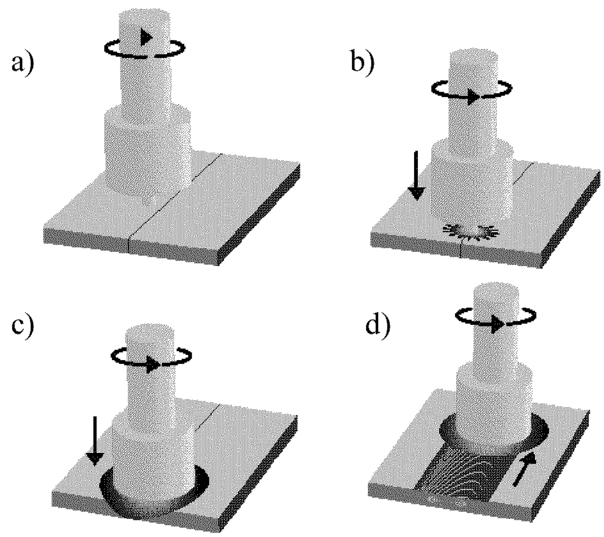

FIGURE 1. Schematic illustration of friction stir welding: a) rotating tool prior to contact with the plate; b) tool pin makes contact with the plate, creating heat; c) shoulder makes contact, restricting further penetration while expanding the hot zone; and d) plate moves relative to the rotating tool, creating a fully recrystallized, fine grain microstructure.

When the shoulder contacts the metal surface, its rotation creates additional frictional heat and helps to plasticize a larger cylindrical metal column around the inserted probe. The shoulder provides a forging force that contains the upward metal flow caused by the tool probe. During welding, the metals to be joined and the tool are moved relative to each other such that the tool tracks the weld interface. The rotating tool provides a continual hot working action, plasticizing metal within a narrow zone. As the tool translates along the joint line, plasticized material is stirred and forged behind the trailing edge of the pin where it consolidates and cools, not solidified, to form a recrystallized fine grain microstructure.

Although melting does not occur during FSW, temperatures are sufficiently high and times at temperature sufficiently long to cause dissolution, nucleation, and/or coarsening of strengthening precipitates. The temperature-time profile changes with distance from the nugget causing a gradient in microstructure and precipitate morphology. The altered microstructure can have corrosion resistant properties significantly different from those of the parent alloy.

EXPERIMENTAL

Material used in this study was 6.35 mm thick AA2024-T351, AA7050-T7651, AA7075-T7651, and AA7075-T651. Samples were friction stir welded using conventional friction stir welding practices[1]. Following welding, samples were tested after naturally aging for five months.

The range in corrosion resistant properties of the various weld zones was determined using several approaches. The degree of sensitization of the FSW material was determined by microscopic examination of specimens after exposure to a 10% dilution composition of the solution used in the ASTM G34 Constant Immersion Exfoliation (EXCO) test. Pitting potentials were measured in deaerated 0.6 M NaCl using the potentiodynamic polarization technique in accordance with ASTM G-61. For these measurements, test samples from the heat affected zone (HAZ) were obtained by cutting parallel to the HAZ/nugget boundary and 0.5 mm into the HAZ. A cut made through the center of the nugget, perpendicular to the weld axis, was used to determine the pitting potential of the nugget. Susceptibility to stress corrosion cracking (SCC) was evaluated using the slow strain rate (SSR) method described in ASTM Standards G-129 and G-49. Tensile specimens were machined transverse to the weld with the gauge section perpendicular to the rolling direction. Gage cross section dimensions were 6.35mm x 3.18mm. The gauge length included the weld nugget and both HAZ's. Specimens, electrically insulated from the grips, were mounted in a 1.5 liter cell. A 0.6M NaCl solution open to the air was continuously recirculated through the cell from a 5 liter reservoir.

RESULTS AND DISCUSSION

Figure 2 is a macrograph of the nugget and the adjacent zones of FSW AA 7050-T7651. This is typical of all of the FSW aluminum alloys investigated. The onion ring appearance is associated with fine bands of very fine grain microstructure (3μm) with a high density of second phase particles alternately dispersed between bands of fine grain microstructure (5μm) with a lower volume fraction of second phase precipitates. The nugget microstructure consists of recrystallized equiaxed fine grains (3 to 5 microns). The FSW process generates zones adjacent to the weld nugget with two different microstructures. A heat affected zone (HAZ) is created a short distance from the weld nugget where the metal has experienced a thermal transient but no deformation. Immediately adjacent to the weld nugget is a partially recrystallized zone (PRZ) where the microstructure has experienced both deformation, as well as the thermal transient. The PRZ in Figure 2 is the region with the redirected grains adjacent to the weld nugget.

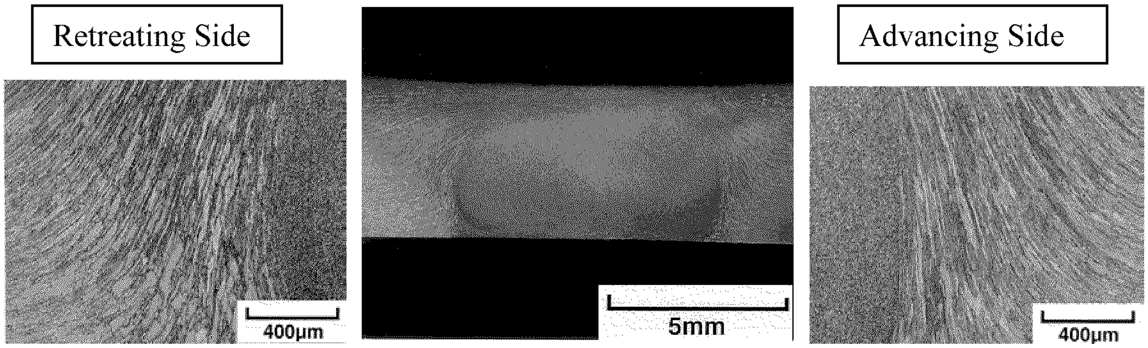

FIGURE 2. Aluminum alloy AA 7050-T7651 following friction stir welding, transverse view in the direction of travel. Nugget has a fine grain fully recrystallized microstructure. A partially recrystallized zone with uplifted grains is adjacent to the nugget.

Earlier work in this program[11-12] and results of others[13-14] demonstrated that FSW sensitizes microstructures in the weld zone of some high strength aluminum alloys. A simple immersion test illustrates weld zone sensitized regions. Figure 3 shows examples of immersion test results on friction stir welded AA2024-T351, AA7050-T7651, and AA7075-T7651. These photomicrographs were taken following exposure to a modified composition of the ASTM G34 EXCO solution used to determine exfoliation resistance. The attack is different for each alloy. Intermetallics are preferentially attacked in the HAZ of AA2024-T351 resulting in deep pits. Intergranular attack occurs in AA7050-T7651 initiating at the nugget/PRZ interface and spreading into the nugget. Intergranular attack also occurs in AA7075-T7651, but it initiates at the PRZ/HAZ interface and spreads into the HAZ.

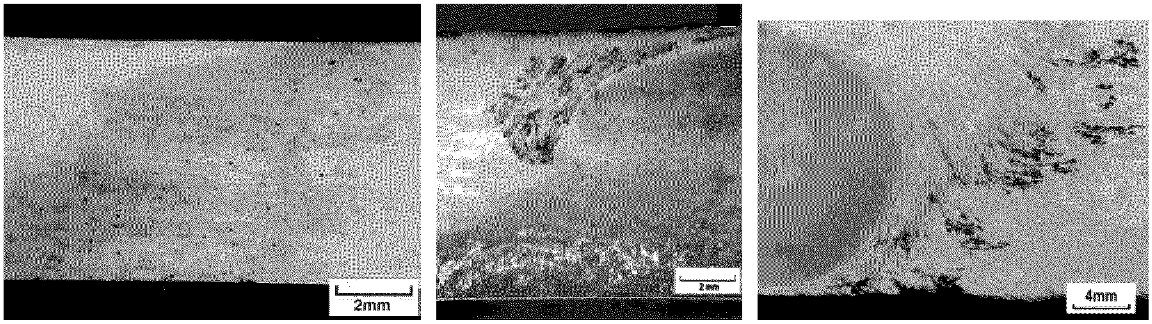

a) AA2024-T351 b) AA7050-T7651 c) AA7075-T7651

FIGURE 3. Attack in the sensitized zones of a) AA2024-T351, b) AA7050-T7651, and c) 7075-T7651 by immersion in modified ASTM G34 EXCO solution.

The results of potentiodymanic polarization in deaerated 3.5% NaCl give additional insights into the effects of FSW on corrosion behavior. These results (Figure 4) show that the pitting potentials in the weld zone are lower than those in the parent metal. In the materials tested, the pitting potential of the HAZ was always the lowest except in AA7050-T7651 where the nugget had the lowest pitting potential. The pitting resistance in the nugget and HAZ of the T7 temper is reduced more than that in the T6 temper.

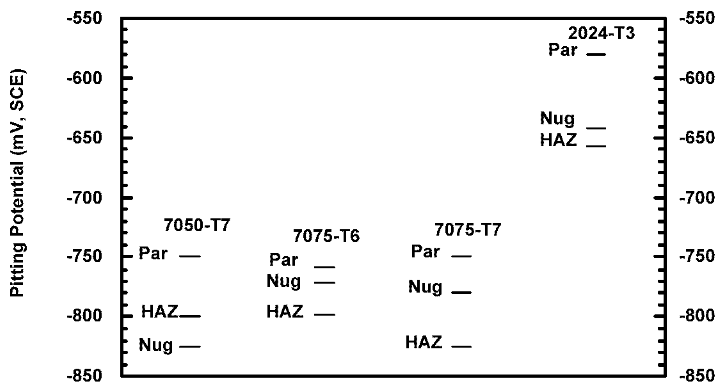

FIGURE 4. Pitting potentials of four high strength aluminum alloys, following FSW, comparing values in the heat affected zone (HAZ) and nugget (Nug), with the parent metal (Par).

The SSR results show that the weld zones of AA7050-T7651 (Figure 5) and AA7075-T7651 (Figure 6) are susceptible to SCC. These measurements, made during exposure to 3.5% NaCl, showed loss of ductility in the FSW materials. Susceptibility to SCC is expressed as the strain rate dependence of the elongation in the NaCl solution. All of the FSW Al alloys tested had strain rate independent elongations in dry air. Both FSW AA7050-T7651 and FSW AA7075-T7651 had the same elongation in air and solution at the highest strain rate used, 3 X 10^{-4} s^{-1}. The elongation of FSW AA7050-T7651 in solution decreased much more rapidly than that of FSW AA7075-T7651 as the strain rate decreased. This suggests that the SCC crack growth rate in FSW AA7050-T7651 is greater than that in FSW AA7075-T7651, and thus more susceptible to SCC. Conversely, the parent material AA7075-T7651 is more susceptible to SCC than the parent AA7050-T7651.

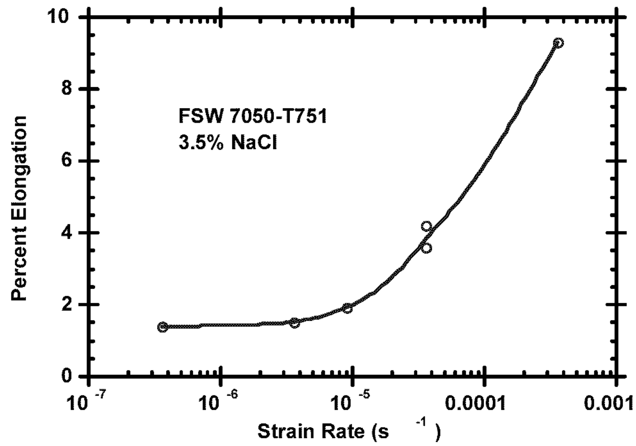

FIGURE 5. Strain rate dependence of the elongation of AA7050-T7651 from the SSR results in 0.6 M NaCl open to the air.

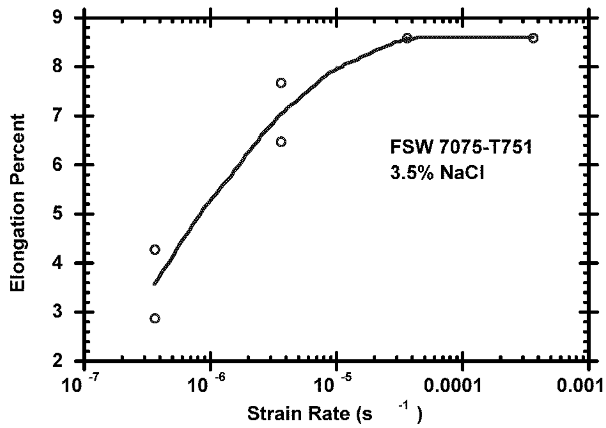

FIGURE 6. Strain rate dependence of the elongation of AA7075-T7651 from the SSR results in 0.6 M NaCl open to the air.

Figure 7 shows an optical cross sectional view of the FSW AA7050-T7651 specimen pulled to failure in solution at a strain rate of 10^{-6} s^{-1} and an SEM view of the fracture surface. The optical macrograph shows a fracture path along the nugget/PRZ interface on the weld advancing side. The SEM micrograph shows an intergranular fracture advancing through the nugget fine grain microstructure. This is consistent with the immersion results illustrating that the most highly sensitized region is the interface between the prz and the nugget. The post-test fractrography for AA7075-T7651 (Figure 8) shows intergranular fracture on the advancing side of the weld in the large grain region of the HAZ. This is again consistent with the immersion tests showing that in this case, the most highly sensitized region is in the HAZ. SEM fracture surface micrographs showed deep grooves on the specimen edges where the elongated grains pulled out when decohesion occurred in the grain boundaries. (The tensile axis is in the long transverse direction). The center of the specimen failed by ductile fracture when failure occurred by overload as the load carrying cross section decreased as the SCC cracks propagated from the edges. As shown in Figure 9, FSW does not decrease the SCC resistance of AA2024-T351 in the 3.5% NaCl solution, but, as discussed above, the HAZ of FSW 2024 is highly susceptible to pitting.

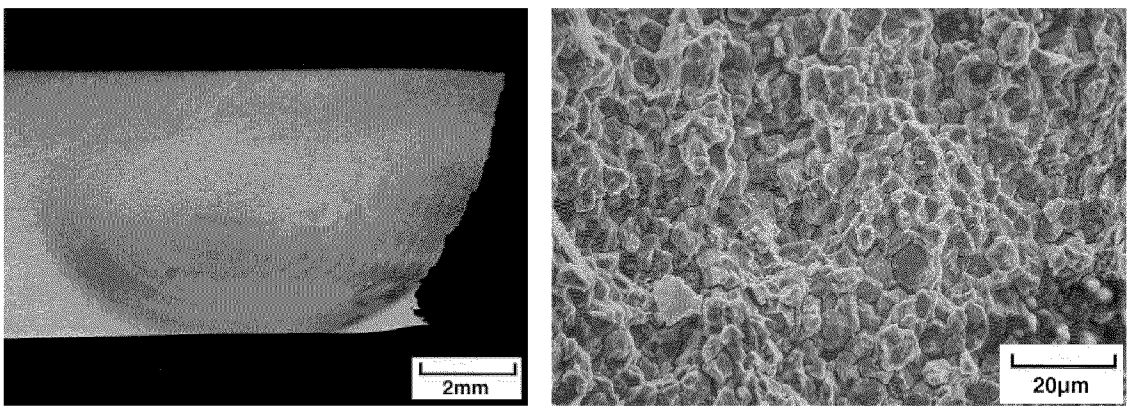

a) b)

FIGURE. 7. SCC fracture in FSW AA7050-T751 a) Optical macrograph showing cross sectional view and b) SEM photomicrograph of the fracture face.

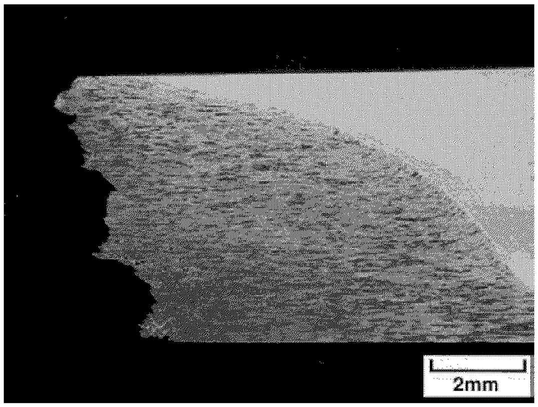

a)

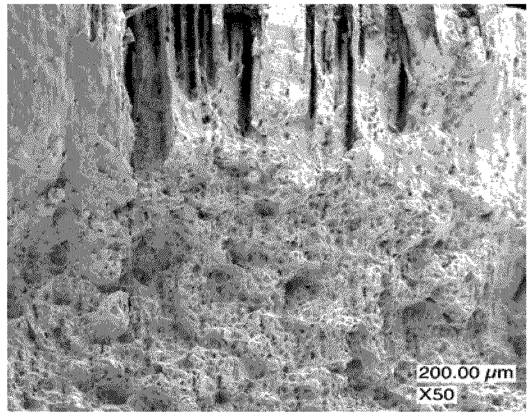

b)

FIGURE 8. SCC fracture in FSW AA7075-T751 a) Optical macrograph showing cross sectional view and b) SEM photomicrograph of the fracture face.

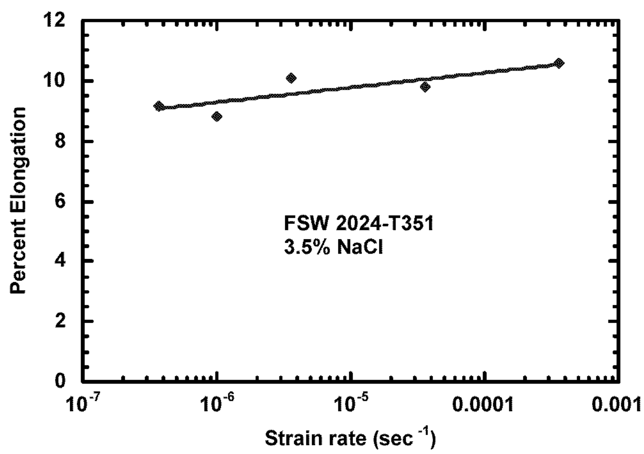

FIGURE 9. Strain rate dependence of the elongation of AA2024-T351 from the SSR results in 0.6 M NaCl open to the air.

In summary, the 2XXX (Al-Cu-Mg) and 7XXX (Al-Zn-Mg-Cu) series high strength aluminum alloys investigated in the program are sensitized by FSW. The results illustrate a strong alloy composition dependence on the sensitization process. Small changes in alloy composition (AA7050-T7 vs. AA7075-T7) cause the location of the sensitized microstructure in the weld zone to change. Large changes in alloy composition can change the type of corrosion attack that occurs in the sensitized microstructure (AA2024 vs. AA7075 and AA7050). The

2XXX and 7XXX alloys derive their high strength from the intermetallic compounds which precipitate either during natural aging at room temperature or artificial aging at intermediate temperatures. The compositions of the precipitates and grain boundaries are changed by the thermal transients generated during FSW. Preliminary analytical electron microscopy measurements of the sensitized microstructures do not conclusively indicate a grain boundary, precipitate free zone, or precipitate chemistry, which correlates with sensitization. These chemistries are complex and vary with distance from the center line of the weld and with alloy.

Six procedures for preventing sensitization or restoring the SCC resistance of FSW precipitation hardened aluminum alloys are being investigated. Active/passive cooling during FSW and the use of Sc as an alloying addition are aimed at preventing composition changes in precipitates and grain boundaries responsible for the sensitized microstructure. Pre/post-weld heat treatment, laser treatment, and friction stir processing of friction stir welds have the potential to restore the corrosion resistance in sensitized weld zones to that of the parent metal. Post weld treatment by low plasticity burnishing (LPB) will change the residual stress if performed after FSW. If LPB is performed prior to FSW, the resulting deformation could alter the deleterious nucleation and growth kinetics of the precipitates during welding.

ACKNOWLEDGEMENT

Support of this work by ONR Contract# N0014-99-C-0153/P00002 is gratefully acknowledged, John Sedriks Program Manager.

REFERENCES

1. W.M. Thomas, et al, "Friction Stir Butt Welding", International Patent Appl. No. PCT/GB92/02203, GB Patent Appl. No. 9125978.8, Dec. 1991, and U.S. Patent No. 5,460,317, (Oct. 24, 1995).

2. C.J. Dawes and W.M. Thomas, *TWI Bulletin 6* (Nov./Dec. 1995): p. 124.

3. M. Ellis and M. Strangwood, *TWI Bulletin 6* (Nov/Dec 1995): p.138.

4. C.J. Dawes and W.M. Thomas, *Welding Journal*, 75, 3 (1996): p. 41.

5. O.T. Midling, "Material Flow Behavior and Microstructural Integrity of Friction Stir Butt Weldments", *Proc. 4th Int'l. Conf. on Aluminum Alloys*, Atlanta GA, (Sept. 1994).

6. M.W. Mahoney, *Welding and Joining*, (Jan./Feb. 1997): p. 18.

7. S. Kallee and D. Nicholas, *Welding and Joining*, ((Feb. 1998): p. 18.

8. C. J. Dawes, *Welding & Metal Fabrication*, (January 1995): p. 14.

9. C.G. Rhodes, M.W. Mahoney, W.H. Bingel, R.A. Spurling, and C.C. Bampton, *Scripta Met*.36 (1997): p 69.

10. M.W. Mahoney, C.G. Rhodes, J.G. Flintoff, R.A. Spurling, and W.H. Bingel, *Metallurgical and Materials Trans.* 29A (July 1998): p. 1955.

11. Jesse Lumsden, Murray Mahoney, Gary Pollock, Doug Waldron, and Angelo Guinasso, "Stress Corrosion Susceptibility in 7050-T751 Aluminum Following Friction Stir Welding", *Proc. First Friction Stir Welding Symposium,* (TWI, London, 1999).

12. Jesse Lumsden, Murray Mahoney, Gary Pollock, Cecil Rhodes, Corrosion 55, 12 (1999): p. 1127.

13. 13. A.J. Leonard, Proceedings of the Third International Symposium on Friction Stir Welding, Kobe, Japan, September, 2001.

14. G.S. Frenkel, Z. Xia, Corrosion, 55 (1999), p. 139.